

## Kinetic hindrance during the initial oxidation of Pd(100) at ambient pressures

E. Lundgren, J. Gustafson, A. Mikkelsen, and J.N. Andersen  
 Department of Synchrotron Radiation Research, Institute of Physics,  
 University of Lund, Box 118, S-221 00 Lund, Sweden

A. Stierle and H. Dosch  
 Max-Planck Institut für Metallforschung, Heisenbergstr.3, D-70569 Stuttgart, Germany

M. Todorova, J. Rogal, K. Reuter, and M. Scheer  
 Fritz-Haber Institut der Max-Planck Gesellschaft, Faradayweg 4-6, D-14195 Berlin, Germany  
 (dated: March 22, 2024)

The oxidation of the Pd(100) surface at oxygen pressures in the  $10^{-6}$  to  $10^3$  mbar range and temperatures up to 1000 K has been studied in-situ by surface x-ray diffraction (SXRD). The results provide direct structural information on the phases present in the surface region and on the kinetics of the oxide formation. Depending on the (T;p) environmental conditions we either observe a thin ( $\sqrt{5} \times \sqrt{5}$ )R27 surface oxide or the growth of a rough, poorly ordered bulk oxide film of PdO predominantly with (001) orientation. By either comparison to the surface phase diagram from first-principles atomistic thermodynamics or by explicit time-resolved measurements we identify a strong kinetic hindrance to the bulk oxide formation even at temperatures as high as 675 K.

PACS numbers: 61.10.-i, 81.65.Mg, 68.55.Jk, 68.43.Bc

Many technologically important materials containing transition metals are intended for use under oxygen pressures much higher than those of the high or ultra high vacuum (UHV) environment typically employed in surface science related investigations of the structural, electronic, and chemical properties of these materials. As the surface properties of such materials may be significantly altered by the oxidation or corrosion [1, 2, 3] occurring at oxygen pressures difficult to achieve in conventional UHV experiments, it is disconcerting that most of our present atomic-scale knowledge derives from such experiments or from theoretical treatments which neglect the surrounding gas-phase. Despite the pressure limitations a few such experiments and theoretical simulations have in recent years significantly advanced our atomic-scale understanding of the initial oxidation of metal surfaces, demonstrating e.g. how radically a surface may change its structure and functionality under conditions appropriate for high pressure oxidation catalysis [1, 2] and how the growth of bulk oxide films is often preceded by the formation of few-atom ic-layer-thin so-called surface oxides of complex geometrical structure and with properties often unknown from the bulk oxides [4, 5, 6]. The unexpected and complex behavior revealed by these experiments emphasizes the need for further in-situ investigations of the structural, electronic and chemical surface properties at higher oxygen pressures but maintaining the accuracy known from UHV studies – in particular to also address the kinetics of oxidation and corrosion processes.

A main reason for the lack of in-situ investigations has been the scarcity of appropriate experimental techniques that provide the aspired atomically-resolved infor-

mation at high pressure in situ, or theories that explicitly include the effect of the surrounding gas-phase. Recently enforced attempts to overcome this limitation have on the theoretical side led to the development of first-principles atomistic thermodynamics, where electronic structure theory calculations are combined with thermodynamic considerations to address the surface structure and composition of a metal surface in equilibrium with arbitrary environments (See Refs. [7, 8] and references therein). On the experimental side the state-of-the-art is, however, currently still characterized by either traditional ex-situ atomic-scale investigations [1], or new high pressure techniques like high pressure scanning tunneling microscopy (STM) that still lack atomic resolution [2].

In this Letter we demonstrate how precise knowledge of the (T;p)-conditions under which such various oxides, -bulk and surface-, exist can be obtained by means of in-situ surface X-ray diffraction (SXRD) measurements. We have chosen to study Pd as the metal is a highly active oxidation catalyst of hydrocarbons under oxygen-rich conditions [9]. Still it is unknown whether Pd or PdO is the active phase [10]. Monitoring the oxidation of the Pd(100) surface over the pressure range from  $10^{-6}$  to  $10^3$  mbar and up to sample temperatures of 1000 K, we observe the formation of both the previously characterized ( $\sqrt{5} \times \sqrt{5}$ )R27 surface oxide [6] and the transform to three-dimensional bulk oxide films. Framing our experimental data with the equilibrium results from atomistic thermodynamics calculations we can identify kinetically inhibited bulk oxide growth even at temperatures as high as 675 K. Under suitable conditions this hindered transformation to the bulk oxide can be followed on a time

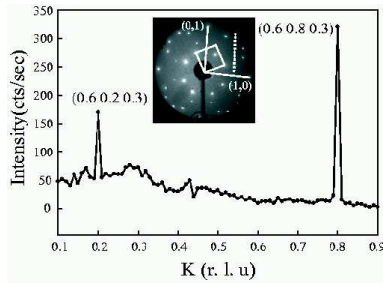


FIG. 1: SXRD in-plane K-scan in reciprocal lattice units (r.l.u.) along (0.6 K 0.3) at  $T = 575$  K and  $p = 10^{-3}$  mbar. The location of this scan line in reciprocal space is indicated in the inset showing the diffraction from the  $(\sqrt{5} \times \sqrt{5})R27$  surface oxide as observed in UHV-LEED. The direction of the in-plane (H K) basis vectors and the unit-cell of one of the surface oxide domains are also plotted in the inset.

scale currently accessible to the experiment, opening the door to time-resolved atomic-scale studies of the initial oxidation process of metal surfaces at ambient pressures.

The SXRD measurements were performed at the Angstrom Quelle Karlsruhe (ANKA) beam line in Germany [11]. A photon energy of 10.5 keV was used and the experiments were conducted in a six-circle diffraction mode. The crystal basis used to describe the (H K L) diffraction is a tetragonal basis set  $(a_1, a_2, a_3)$ , with  $a_1$  and  $a_2$  lying in the surface plane and of length equal to the nearest neighbor surface distance  $a/\sqrt{2}$ , and  $a_3$  out-of-plane with length  $a$  ( $a(\text{Pd}) = 3.89 \text{ \AA}$ ). The UHV x-ray diffraction chamber allowed partial oxygen pressures of up to  $10^3$  mbar, and the temperature was estimated from a thermocouple mounted behind the transferable sample holder, resulting in an uncertainty of the sample temperature of  $\pm 25$  K. The sample and the cleaning procedure are identical to the one described in an earlier UHV study [6]. The oxide films grown were found to be metastable on the time scale of hours under UHV conditions, and could readily be desorbed at 1175 K.

The atomistic thermodynamics results are based on density-functional theory (DFT) calculations performed within the Full-Potential Linear Augmented Plane Wave (FP-LAPW) scheme [12] using the generalized gradient approximation (GGA) [13] for the exchange-correlation functional. The supercell setup and the highly converged basis-set [14] have been detailed in our preceding study [6]. To determine the range of (T; p)-conditions in which this surface oxide would represent the thermodynamically most stable state, we evaluate the Gibbs free energy of adsorption [7, 8] and compare it to other possible states of the system, like the reported  $p(2 \times 2)$  on-surface phase with O in fcc sites [6, 15] or the tetragonal PdO bulk oxide [16].

Figure 1 depicts a SXRD K-scan at a sample temperature of 575 K and partial oxygen pressure of  $10^{-3}$  mbar. From the inset showing the reciprocal space as observed

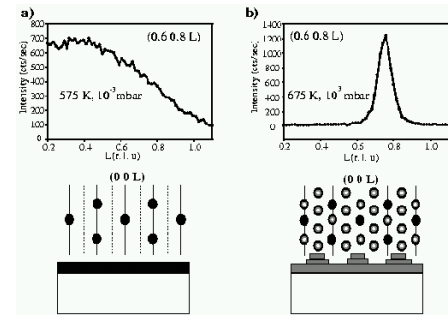


FIG. 2: Top: SXRD out-of-plane L-scan along (0.6 0.8 L). Bottom: corresponding schematic of the observed out-of-plane diffraction (full lines – rods due to both Pd(100) and the surface oxide, dashed lines – rods only due to the surface oxide. Bragg reflections from bulk Pd and bulk PdO are marked as black and grey circles respectively). a)  $p = 10^{-3}$  mbar and  $T = 575$  K, only the surface oxide diffraction is apparent, b)  $p = 10^3$  mbar and  $T = 675$  K, diffraction is now due to a bulk-like PdO film.

with UHV low-energy electron diffraction (LEED) it is obvious that the two observed peaks in the SXRD scan arise from the  $(\sqrt{5} \times \sqrt{5})R27$  surface oxide. The width of the rocking scan at the (0.6 0.8 0.3) reflection is (0.13) equal to the substrate rocking scan in the minimum of the crystal truncation rod (CTR) before dosing, allowing us to conclude that the surface oxide domains extend over complete substrate terraces (in agreement with our previous STM results [6]).

The out-of-plane diffraction from the (0.6 0.8 L) reflection under the same temperature and pressure conditions is shown as an L-scan in the top section of Fig 2a. The smooth decrease of the intensity and the absence of sharper peaks with increasing L is a clear fingerprint of a single diffracting layer, in agreement with the recent finding [6] that the  $(\sqrt{5} \times \sqrt{5})R27$  surface oxide consists of a single PdO (101) layer adsorbed on the Pd(001) surface. The observed diffraction changes significantly as the oxygen pressure and temperature is increased to  $10^3$  mbar and 675 K, respectively, as shown in Fig. 2b. Instead of a smoothly decreasing diffraction intensity with increasing L, a peak is now observed at  $L = 0.74$ . Since the reciprocal lattice is defined by the lattice constant of Pd, this peak corresponds to a lattice distance of  $a(\text{Pd})/0.74 = 5.26 \text{ \AA}$ , which is very close to the c-lattice constant of bulk PdO, namely 5.33 Å. Thus, we observe bulk-like diffraction from PdO, indicating the formation of several layers of PdO on the Pd(001) surface. Interestingly, we also note that no diffracted intensity is observed at  $L = 0$  anymore demonstrating that the  $(\sqrt{5} \times \sqrt{5})R27$  surface oxide has completely disappeared from the surface, i.e. the initially formed PdO (101) plane does not continue to grow but instead restructures. This is in agreement with our DFT calculations identifying the (101) orientation as a higher-energy facet of PdO [6], and also with experi-

mental observations on the preferred growth direction of PdO [17]. Further, since no finite thickness oscillations are observed along the rod, the observed oxide film must be rough, as has also been reported in a recent high-pressure STM study of this surface [18].

A more detailed analysis of our diffraction data allows us to even draw some more quantitative conclusions about the properties of the grown oxide. We observe no change in the overall shape of the (1 1 L) CTR upon oxidation. Without apparent relaxation, we therefore attribute the change in integrated intensity at them inum (1 1 1) to a change in surface roughness. Estimating the latter within the model [19] yields approximately root-mean-square roughness of 10 Å, whereas the measured width of 0.1 of the  $L=0.74$  peak indicates an average film thickness of around  $3.89 \text{ Å} / 0.1 = 40 \text{ Å}$ . The poor order of the formed oxide fringe is further reflected in the 1 width of the rocking scan at the  $L=0.74$  peak, indicating either an enhanced mosaic spread, or a small domain size of the PdO at the surface, which would comply with the previous STM observations by Hendriksen et al. [18]. This poor order is probably also reflected by our inability to detect reflections from the O sublattice. In fact, the (0.6 0.8 0.74) peak corresponds to the (1 0 1) reflection in PdO bulk coordinates. In addition to this reflection we also found the (103), (200) and the (202), and equivalents when rotating by 90 degrees. By observing that this indexing is similar to the selection rule for a bcc lattice for which the sum of all indices must be even, we conclude that what we observe is the Pd sublattice in PdO, which forms a distorted bcc lattice. The orientation and geometry of the ordered domains are then predominantly PdO (001) kPd (100).

Having thus established the means to distinguish and characterize the formation of either surface or thicker oxide films at higher O partial pressures from the diffraction signals, we may in a straightforward way construct a diagram showing which phase we measure under which (T;p)-conditions. The result is shown in Fig. 3, covering the whole range of now experimentally accessible gas pressures from  $10^{-6}$  mbar to ambient pressure. Most strikingly, the  $(\sqrt{5} \times \sqrt{5})R27^\circ$  structure is found under a wide variety of conditions (even at an oxygen pressure of  $10^3$  mbar and a sample temperature of 575 K we still observe only the formation of this surface oxide and no indications for the growth of a thicker oxide film on the time scale of 1 hr currently accessible to the experiment).

As a first step to understand this data we proceed by comparing it with the surface phase diagram obtained by DFT and atomistic thermodynamics. Figure 3b gives the corresponding (T;p)-diagram, showing which phase would be most stable on the basis of our DFT data, if the surface were in full thermodynamic equilibrium with the surrounding oxygen gas phase. We immediately stress that although state-of-the-art, some approximations like e.g. the present treatment of vibrational contributions

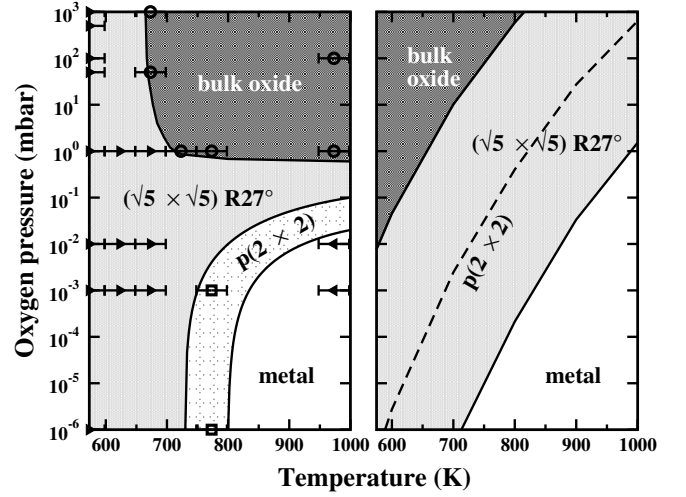


FIG. 3: Left: (T;p)-diagram showing the measured phases in the whole range of experimentally accessible conditions from UHV to ambient pressure. The "phase boundaries" (see text) are rough estimates to guide the eye. Right: Corresponding surface phase diagram, as calculated by first-principles atomistic thermodynamics (see text). The dashed line indicates the thermodynamic stability range of the  $p(2 \times 2)$  adphase, if formation of the surface oxide was kinetically inhibited.

to the free energies, as well as the uncertainty introduced by finite basis set and the employed exchange-correlation functional may well allow for errors in the phase boundaries of the order of 100 K and (depending on temperature) of up to several orders in pressure [7, 8].

Taking this into account we notice a gratifying overall agreement between theory and experiment in this wide range of environmental conditions. At a closer look there is, however, a notable difference that is beyond the uncertainties underlying both the experimental and theoretical approach: the experimental observation of the  $(\sqrt{5} \times \sqrt{5})R27^\circ$  surface oxide in the top left corner of the drawn diagram, i.e. at lower temperatures and high pressures. Since the central assumption of theory, which predicts the stability of the bulk oxide under such conditions, is the full thermodynamic equilibrium between surface and gas phase, we interpret this difference as reflecting kinetic limitations to the growth of the bulk oxide under such conditions. This is also apparent even within the experimental data set alone. If the surface was fully equilibrated with the environment, the evaluated phase boundaries would have to follow lines of constant oxygen chemical potential, which is the single determining quantity if thermodynamics applies. In the drawn (T;p)-plots such lines of constant chemical potential would always be parallel to the phase boundaries as drawn in the theoretical diagram, cf. Fig. 3b, which the bulk/surface oxide boundary drawn in Fig. 3a (even considering all uncertainties) is clearly not. Similarly we also understand the experimental observation of the  $p(2 \times 2)$  adsorbate phase,

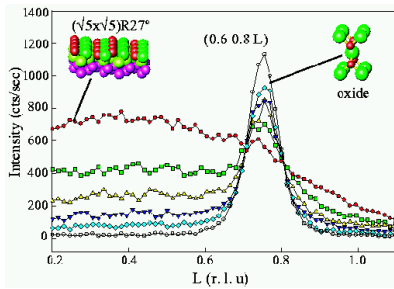


FIG. 4: Six consecutive L-scans along  $(0.6\ 0.8\ L)$  at 675 K and 50 mbar. Each scan took 240 sec to record, showing the gradual transformation from the diffraction signal characteristic of the surface oxide to the one of the bulk oxide, cf. Fig. 2. Solid circles: first spectrum; empty circles: last spectrum taken.

which according to theory is never a thermodynamically stable phase, as a sign of kinetic hindrance to the formation of the  $(\sqrt{5}\times\sqrt{5})R27^\circ$  phase. Correspondingly, we have also marked in the theoretical plot the area, where the  $p(2\times 2)$  would turn out more stable than the clean surface, if the surface oxide can not form.

Under suitable conditions we can even follow the kinetically limited transition from surface to bulk oxide within the time resolution of our current experiment. This is illustrated in Fig. 4 showing how the diffraction signal at 675 K and  $p = 50$  mbar slowly transforms at every consecutive scan from the one characteristic for the surface oxide phase, cf. Fig. 2a, to the one of the bulk oxide film, cf. Fig. 2b. Obviously, this transformation will be faster for higher temperatures, so that we immediately observe the bulk oxide, or eventually so slow at lower temperatures that we can no longer measure the transition within the time frame open to our experiment. In passing we naturally note that these clear kinetic limitations at time scales of 1 hr even at technologically relevant temperatures as high as 675 K, are somewhat at variance with the well-known theoretical notion by King and coworkers suggesting that oxide growth should immediately set in as soon as it is thermodynamically possible [20].

In conclusion we have studied the oxidation of the Pd(100) surface from  $10^{-6}$  mbar to ambient pressure by in-situ SXRD. Depending on the environmental conditions we observe either the formation of the  $(\sqrt{5}\times\sqrt{5})R27^\circ$  surface oxide (essentially a well-ordered layer of PdO (101)), or the growth of  $\sim 40$  Å poorly ordered and rough PdO bulk oxide, predominantly with PdO (001) orientation. The range of  $(T;p)$ -conditions where we measure the surface oxide is surprisingly large, and goes for  $T < 600$  K even up to ambient pressures. Compar-

ing with the theoretical surface phase diagram from first-principles atomistic thermodynamics we interpret this as reflecting a kinetic hindrance to the formation of the bulk oxide, which is clearly an activated process due to the involved massive restructuring at the surface. Such kinetic limitations in the initial oxide formation process have hitherto barely been addressed, but could be crucial for understanding high pressure applications like e.g. oxidation catalysis. Our measurements demonstrate the usefulness of SXRD for the study of the oxidation process of almost any material in such high pressure environments, providing the aspired atomically resolved structural information of any thin film or nano-based structure exposing its surface to an ambient working atmosphere.

This work was financially supported by the Swedish Natural Science Council and the DFG -priority program "Realkatalyse".

---

Electronic address: edvin.lundgren@sljus.lu.se

- [1] H. Over et al, Science 287, 1474 (2000).
- [2] B. L. M. Hendriksen and J. W. M. Frenken, Phys. Rev. Lett. 89, 046101 (2002).
- [3] C. Stamp et al, Surf. Sci. 500, 368 (2002).
- [4] C. I. Carlisle et al, Phys. Rev. Lett. 84, 3899 (2000).
- [5] E. Lundgren et. al, Phys. Rev. Lett. 88, 246103 (2002).
- [6] M. Todorova et al, Surf. Sci. 541, 101 (2003).
- [7] K. Reuter and M. Scheer, Phys. Rev. B 65, 035406 (2002).
- [8] W.-X. Li, C. Stamp and M. Scheer, Phys. Rev. Lett. 90, 256102 (2003).
- [9] M. Ziauddin, G. Veser and L. D. Schmitz, Catal. Lett. 46, 159 (1997).
- [10] G. Veser, A. Wright, and R. Caretta, Catal. Lett. 58, 199 (1999).
- [11] <http://hikwww1.fzk.de/iss/beamlinebook.html>
- [12] P. Blaha, K. Schwarz and J. Luitz, WIEN 97, Techn. Universität Wien, Austria, (1999). ISBN 3-9501031-0-4.
- [13] J. P. Perdew, K. Burke and M. Ernzerhof, Phys. Rev. Lett. 77, 3865 (1996).
- [14] FP-LAPW basis set parameters:  $R_{MT}^{pd} = 1.8$  bohr,  $R_{MT}^o = 1.3$  bohr,  $l_{max}^f = 12$ ,  $l_{max}^{pot} = 4$ ,  $E_{wf}^{max} = 20$  Ry,  $E_{pot}^{max} = 169$  Ry, and a  $(4\times 4\times 1)$  Monkhorst-Pack grid with 28 k-points in the full Brillouin zone.
- [15] G. Zheng and E. I. Altman, Surf. Sci. 462, 151 (2000).
- [16] D. Rogers, R. Shannon and J. Gillson, J. Solid State Chem. 3, 314 (1971).
- [17] J. McBride, K. Hass and W. Weber, Phys. Rev. B 44, 5016 (1991).
- [18] B. L. M. Hendriksen et al, Surf. Sci. (submitted).
- [19] I. K. Robinson, Phys. Rev. B 33, 3830 (1986).
- [20] C. I. Carlisle et al, Surf. Sci. 470, 15 (2000), and references therein.